# Development of facilitated transport membranes composed of a dense gel layer containing CO2 carrier formed on porous cylindrical support membranes

Kamio, Eiji
Kasahara, Shohei
Moghadam, Farhad
Matsuyama, Hideto

(Citation)
Chemical Engineering Research and Design,153:284-293

(Issue Date)
2020-01

(Resource Type)
journal article

(Version)
Accepted Manuscript

(URL)
https://hdl.handle.net/20.500.14094/90006810

# Development of facilitated transport membranes composed of a dense gel layer containing $CO_2$ carrier formed on porous cylindrical support membranes

Eiji Kamio[a,*], Shohei Kasahara[a], Farhad Moghadam[b] and Hideto Matsuyama[a,*]

a: Research Center for Membrane and Film Technology and Department of Chemical Science and Engineering, Kobe University, 1-1 Rokkodai-cho, Nada-ku, Kobe, Hyogo 657-8501, Japan.
b: Department of Energy Engineering, Hanyang University, Seoul 04763, Republic of Korea

* Corresponding author: e-kamio@people.kobe-u.ac.jp, matuyama@kobe-u.ac.jp

Key Words: Facilitated transport membrane, $CO_2$ separation, Porous support membrane, Gel layer

## Abstract

It is well known that facilitated transport membranes (FTMs) containing $CO_2$ carriers have high $CO_2$ permeability and excellent permselectivity of $CO_2$ over other light gases. The major challenge in developing FTMs for practical applications is the formation of a separation layer containing $CO_2$ carriers on a support membrane. In this research, we prepared composite membranes by forming a dense gel layer containing glycine as the $CO_2$ carrier on polysulfone (PSf) and ceramic (α-alumina) support membranes. Because of the smaller pore size of the PSf support membrane, the gel layer formed on the PSf membrane was thinner and had higher $CO_2$ permeance than that formed on the alumina membrane. However, the $CO_2$ permeabilities of the FTMs formed on the two support membranes showed different temperature dependences; the FTM formed on PSf membrane had higher $CO_2$ permeability at elevated temperatures of more than ca. 350 K and lower $CO_2$ permeability at low temperatures up to ca. 350 K than the FTM formed on alumina support. The different temperature dependences on the $CO_2$ permeability resulted from the different properties of the gel layer formed on the support membranes. Improvement of the $CO_2$ permeability of FTMs could be enabled by selecting an adequate support membrane.

# 1. Introduction

Membrane technology has attracted intense interest in postcombustion carbon capture as a feasible alternative to conventional amine-based $CO_2$ absorption units (Baker, 2012). Polymers are widely used materials in the industry for gas mixture separations, such as oxygen/nitrogen, hydrogen recovery, and natural gas sweetening (Baker, 2002). However, the application of polymer-based membranes for $CO_2/N_2$ separation is limited by intrinsic trade-off behavior, known as Robeson upper bound (Robeson, 2008). To overcome this limitation, facilitated transport membranes (FTMs) have been introduced as a promising candidate providing both high $CO_2$ permeability and $CO_2/N_2$ selectivity due to the reversible reaction between $CO_2$ and reactive amine-based carriers (Kim et al., 2004; Matsuyama et al., 1999; Rafiq et al., 2016; Tong and Ho, 2017). FTMs containing a mobile carrier showed better performance in terms of $CO_2$ permeability and $CO_2/N_2$ selectivity than fixed-carrier-based FTMs due to the high diffusivity of the $CO_2$–mobile carrier complex through the membrane matrix (Chen and Ho, 2016; Chen et al., 2016; Han et al., 2018). There are abundant studies on the fabrication of FTMs for $CO_2/N_2$ (Deng et al., 2009; Matsuyama et al., 2001; Moghadam et al., 2017b), $CO_2/CH_4$ (Deng and Haegg, 2010), and $CO_2/H_2$ (Zhao and Ho, 2012) separation, demonstrating high $CO_2$ permeation of FTMs, with respect to polymeric membranes. In our group, a new type of FTM was fabricated by incorporating diaminopropionic acid (DAPA), as $CO_2$ carrier, into the polyacrylic acid-polyvinyl alcohol (PAA/PVA) copolymer matrix, which exhibited high $CO_2$ permeance ($3\times10^{-4}$ to $1\times10^{-4}$ mol/m$^2$ s kPa) along with extraordinary $CO_2/H_2$ selectivity between 100 and 400 at elevated temperature (120 to 160 °C) under humid conditions (Yegani et al., 2007). Such a high $CO_2/H_2$ selectivity was mainly attributed to the chemical complex formation between DAPA and $CO_2$ while $H_2$ permeated through the membrane based on solution-diffusion mechanism. Of particular note, the water content in feed gas was found as a key parameter to achieve such high $CO_2$ permeance and $CO_2/H_2$ selectivity.

Generally, the gas permeance of a membrane, which is defined as the gas flux across the membrane normalized by partial pressure difference of the target gas between the membrane, is a key factor to reduce the cost of separation in a membrane-based separation system. Unlike gas permeability, which is a normalized permeance by membrane thickness and an intrinsic property of membrane material, permeance is a membrane characteristic that can be controlled by manipulating the film thickness. Typical commercial membranes used for gas and liquid separations are made from a thin selective layer coated on a porous support, called thin-film composite (TFC) membranes (Baker, 2012; Baker and Low, 2014). To achieve high permeance, a selective layer in TFC membrane should have both high permeability and low thickness. The support used for fabrication of TFC membranes is generally made in the flat sheet or hollow fiber configuration, which of the latter is desired due to its high surface-to-volume ratio (Baker, 2012; Baker, 2002). In addition, interfacial interaction of support (polymeric or inorganic) with a coated selective layer may impact the separation performance of TFC membranes. Regarding their high $CO_2$ permeability, fabrication of a thin layer of FTMs on a porous substrate can afford high-$CO_2$-permeance TFC membranes. Ho *et al.* fabricated high-$CO_2$-permeance FTMs by coating polyvinylamine (PVAm)/piperazine glycinate (PG) solution on the polyether sulfone (PES) substrate (Chen and Ho, 2016). For PVAm/PG TFC membrane with 150 nm thickness, $CO_2$ permeance of 930 GPU (1 GPU = $1\times10^{-6}$ $cm^3$(STP)/($cm^2$ s cmHg)), $CO_2$ permeability of 140 barrer (1 barrer = $1\times10^{-10}$ $cm^3$(STP)cm/($cm^2$ s cmHg)) and $CO_2/N_2$ selectivity of more than 154 was obtained (Chen and Ho, 2016). In subsequent work, PVAm/PG selective layer was cast on a zeolite-Y(ZY) coated PES support to make TFC membrane with $CO_2$ permeance of 800 GPU and $CO_2/N_2$ selectivity of 157 (Wu et al., 2018). Kim *et al.* fabricated PVAm/polysulfone (PSf) composite membranes and claimed that $CO_2$ permeation properties are largely affected by the water content in feed gas and also pH values of the casting solution (Kim et al., 2013). They claimed that higher content of water (i.e., high relative humidity) play two distinctive roles. First, water dissolved $CO_2$ and formed carbamic acid and subsequently bicarbonate, which partially facilitated the $CO_2$ permeation. It also swelled PVAm network and therefore, increase the free volume of the membrane, giving rise to the enhanced diffusivity coefficient of $CO_2$-carrier complexes (Kim et al., 2013). The relative humidity (RH) of the feed gas showed a similar impact on the $CO_2/N_2$ (Deng et al., 2009) and $CO_2/CH_4$ (Deng and Haegg, 2010) transport properties of PVAm/PVA blend TFC membranes. The aforementioned studies mainly investigated the effect of water content, swelling degree of polymer, temperature and $CO_2$ partial pressure on transport properties of FTMs. However, support may influence $CO_2$ gas transport properties of TFC-FTMs. In particular, most of the polymers used for the fabrication of FTMs swell a lot under humid condition (become hydrogel) and therefore, interfacial interaction of selective layer with support may play an important role in achieving high $CO_2$-separation performance.

In this study, we aimed to develop TFC-FTMs on cylindrical support membranes and to investigate the effect of support on $CO_2$ transport properties of PAA/PVA FTM containing glycine as $CO_2$ carrier. PSf and alumina supports were used in this study. The thickness of PAA/PVA selective layer containing glycine, which was coated on the supports, was preferentially adjusted. Effect of temperature on $CO_2$ permeabilities of the PAA/PVA FTMs coated on two types of support was also examined to investigate the different $CO_2$ transport properties of the FTMs formed on different support membranes.

## 2. Experimental

### *2.1. Fabrication of cylindrical membrane with dense gel layer with $CO_2$ separation function*

Glycine was used as a $CO_2$ carrier because it was reported in several studies that amino acid salts can act as a powerful $CO_2$ carrier (Chen et al., 2016; El-Azzami and Grulke, 2009; Kasahara et al., 2012a, b; Moghadam et al., 2017a; Moghadam et al., 2015; Qin et al., 2016). CsOH was used to neutralize the amino group of glycine. Glycine and CsOH were purchased from Wako Pure Chemical Industries, Ltd. (Japan) and used without purification. A polyacrylic acid-polyvinylalcohol (PAA/PVA) copolymer, supplied from Kyodo Yakuhin Co. Ltd., Japan, was used as the gel network.

By vigorously stirring 2 g of PAA/PVA copolymer particles and 80 g of Milli-Q water at room temperature for 5 days or more, the PAA/PVA copolymer particles became fully swollen hydrogel particles and uniformly dispersed hydrogel particle suspension was prepared. Thereafter, 2.93 g of glycine and 5.84 g of CsOH were added to the prepared gel particle suspension. The suspension was vigorously stirred for 1 day or more to completely dissolve glycine and CsOH and impregnate the dissolved glycine and CsOH into hydrogel particles. The obtained hydrogel particle suspension was filtered using cylindrical porous support membranes to form a hydrogel particle deposition layer (gel layer) on the porous support membrane.

In this study, the support membranes used to form the gel layer were an α-alumina support membrane and a polysulfone (PSf) support membrane. The alumina support membrane was purchased from NOK Corporation (Japan). The inner, outer, and average pore diameters of the alumina support membrane were 2.0 mm, 3.0 mm and 100 nm, respectively. The PSf support membrane was provided by Kuraray Co., Ltd. (Japan). The inner diameter, outer diameter, and molecular weight cutoff were 2.0 mm, 2.8 mm, and 13 kDa, respectively.

As mentioned above, the dense gel layer containing the $CO_2$ carrier was formed by depositing hydrogel particles on the inner surface of the alumina and PSf support membranes. In general, dip coating is a simple technique for forming a thin polymer layer on the outer wall of a hollow fiber membrane. However, it is not easy to form a gel layer on the inner wall of a thin hollow fiber membrane via dip coating method. In addition, because the gel layer is sticky, the hollow fiber membranes having the gel layer on the outer surface stick with each other in the module. On the other hand, hollow fiber membranes with gel layers on the inner wall do not stick with each other. We can easily produce a module containing hollow fiber membranes with a gel layer on the inner wall. Therefore, in this study, we developed a method to form the gel layer on the inner wall of the hollow fiber membrane. Fig. 1 shows the schematic illustration of the apparatus used to form the gel layer on the cylindrical support membranes. First, the cylindrical support membrane was inserted in the gas permeation test cell (Fig. 2), and both ends of the support membrane were firmly fixed using an O-ring. In this study, observation of the cross-section of the composite membrane was one of our important investigations. So we adopted an O-ring sealing to easily remove the membrane from the cell after forming the gel layer. In the case of using a PSf support membrane, stainless steel tubes were inserted at both ends of the cylindrical PSf membrane to prevent the PSf support membrane from being deformed, by tightening with an O-ring and closing the channel of the cylindrical membrane. The gas permeation test cell with the cylindrical support was attached to the apparatus for the gel layer formation (Fig. 1). Then, by using a syringe, approximately 5 $cm^3$ of the prepared hydrogel particle suspension was filled in the inside of the cylindrical porous support membrane and the gel particle suspension reservoir. After closing the two-way valves 1, 2, and 3, the trap was filled with $N_2$ gas at the desired pressure. The pressure of $N_2$ gas was adjusted using a back-pressure valve. After the pressure increased to the target value, the two-way valve 2 was opened to perform constant pressure filtration of the gel particle suspension with the cylindrical support membrane. During constant pressure filtration, the filtrate was continuously discharged by circulating $N_2$ gas from the side pipe of the gas permeation cell. By filtrating the hydrogel particle suspension for a predetermined period, the gel particles were deposited on the inner surface of the cylindrical membrane, and a gel particle deposition layer (cake layer) was formed on the inner surface of the cylindrical membrane. After the predetermined time had passed, the pressure was rapidly reduced to an absolute pressure of approximately 200 kPa(A) (hereafter the unit of absolute pressure was expressed as kPa(A)) by opening the back-pressure valve. Thereafter, the two-way valve was immediately opened to discharge the remaining gel particle suspension. Finally, the gas permeation cell was removed from the apparatus and dried for more than 1 h in a thermostat oven, at a constant temperature of 353 K. The composite membrane without glycine and CsOH in the gel layer was also prepared in the same manner except for using the 2.0 g-PVA/PAA gel particle suspension in 80.0 g Milli-Q water dissolved no glycine and CsOH. The gel layer without $CO_2$ carrier was formed on an alumina support by applying 300 kPa(A) for 20 min.

The coating experiment was conducted to evaluate the difference in the structures of gel layers formed under different conditions using different support membranes. In the coating experiment, the effect of the types of support membrane and the applied pressure on the flux of the aqueous phase of the gel particle suspension was evaluated. As described above, in the preparation of a cylindrical membrane with a gel layer, constant pressure filtration of gel particles by the support membranes was performed by applying pressure to the gel particle suspension filled in the porous support membranes. By carrying out constant pressure filtration for a certain period of time, the aqueous phase was permeated through the support membrane and a cake layer of the gel particles was formed on the inner surface of the support membrane. The permeated solution was recovered, and its weight was measured. The applied pressures were 500 and 600 kPa(A), and the permeated water was collected every 3, 6, 9, 12, 15, and 20 min. When using the gel particle suspension used to prepare the membrane for the gas separation test, a sufficient amount of the permeate was not obtained, so a 10-fold diluted gel particle suspension was used in the coating experiment.

During the drying process, $N_2$ gas was flowed inside and outside the cylindrical membrane. The thickness of the gel layer formed on the inner surface of the cylindrical support membrane was determined by observing the cross section of the cylindrical supporting membrane with the gel layer using a field-emission scanning electron microscope (FE-SEM JSM-7500F, JEOL Ltd., Japan).

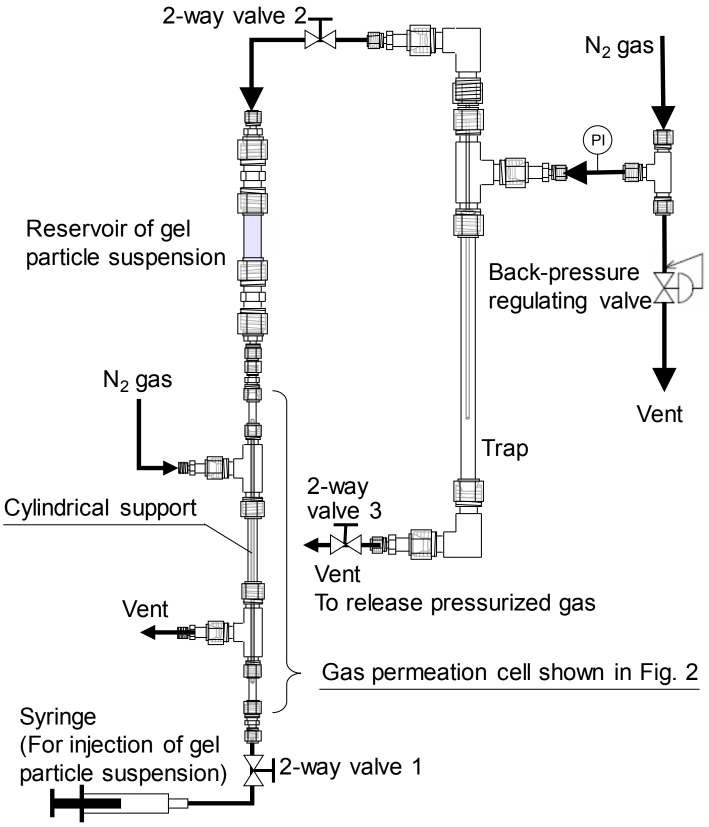

Fig. 1 – Illustration of the experimental setup for formation of dense gel layer on inner surface of a cylindrical support membrane

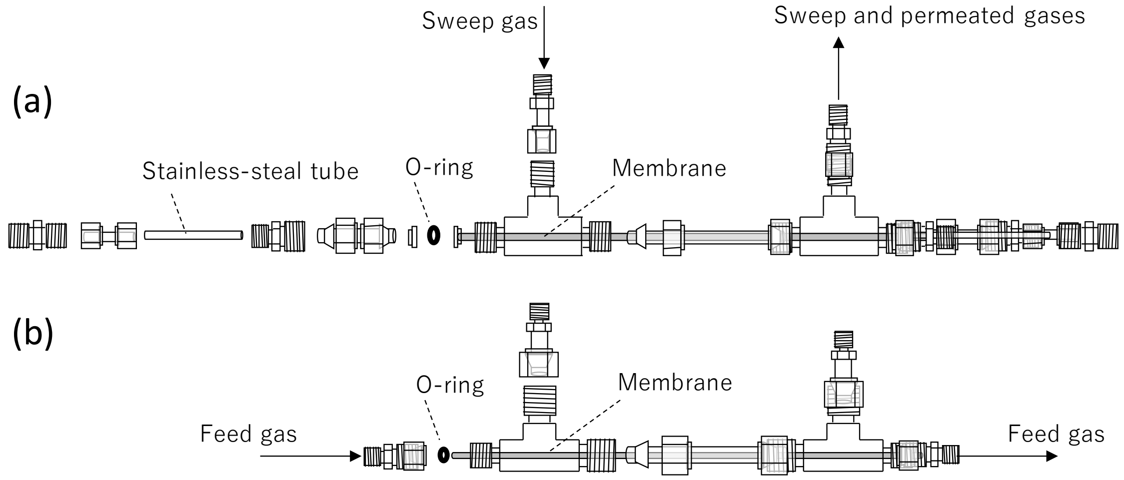

Fig. 2 – Illustration of the gas permeation cell for the evaluation of the gas permeation performances of the cylindrical membrane with a dense gel layer, (a) for the membrane with PSf support membrane and (b) for the membrane with alumina support membrane.

*2.2. Evaluation of gas permeation performances of the cylindrical membranes with gel layer*

The $CO_2$ and $N_2$ permeabilities of the cylindrical membranes with gel layer were measured using the apparatus shown in Fig. 3. The gas permeation cell shown in Fig. 2 having the prepared membrane with an effective permeation area of 4.1 $cm^2$ was placed in a thermostat oven (Yamato Scientific Co., Ltd., Japan). The apparatus equipped mass flow controllers (Hemmi Slide Rule Co., Ltd, Japan.) to adjust the flow rates of $CO_2$, $N_2$, and He. A mixture of $CO_2$ and $N_2$ containing 10 vol% of $CO_2$ and 90 vol% of $N_2$ in a dry basis was mixed with water vapor, which was generated using a vaporizer, and introduced to the lumen side of the cylindrical membrane. The total flow rate of the humid gas was 196 $cm^3$/min. To the shell side of the gas permeation cell, He gas was supplied as the sweep gas at a flow rate of 20 $cm^3$/min. The feed and sweep gases were heated with coiled heat exchangers before introduction to the gas permeation cell. The pressure of the feed and permeate sides was maintained at atmospheric pressure. To determine the composition of the permeated $CO_2$ and $N_2$, the sweep gas containing the $CO_2$ and $N_2$ permeated through the membranes was fed to a gas chromatograph (GC) (GC-8A, Shimadzu Co., column: activated carbon, 1 m). To verify the steady state, each gas permeation test was conducted for 3 h or more until the difference between successive $CO_2$ and $N_2$ peak areas of the GC measurement became less than 1%. The experimental conditions are summarized in Table 1. In this study, effect of temperature on the $CO_2$ and $N_2$ permeances of the composite membranes with different porous supports and various gel layer thicknesses were investigated.

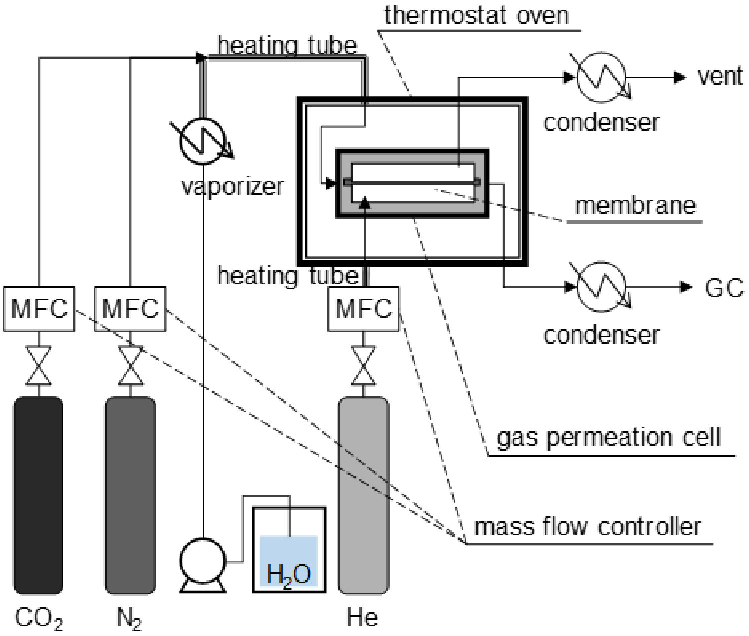

Fig. 3 – Illustration of the experimental setup to measure the gas permeation performances of the membranes. MFC: mass-flow controller, GC: gas chromatograph

Table 1 – Experimental conditions for the gas permeation tests

| Conditions | | Gas | |
|---|---|---|---|
| Temperature | | | 333–373 K (every 10 K) |
| Pressure | | Feed | atmospheric |
| | | Sweep | atmospheric |
| Pressure difference | | | 0 kPa |
| Gas flow rate | | | |
| | Feed | $CO_2$ | 16 $cm^3$/min (8.2 vol%) |
| | | $N_2$ | 144 $cm^3$/min (73.4 vol%) |
| | | Water vapor | 36 $cm^3$/min (18.4 vol%) |
| | Sweep | He | 40 $cm^3$/min |
| | | Water vapor | 0 $cm^3$/min (dry) |

## 3. Results and discussion

### *3.1. Formation of gel layer on the porous support membranes*

The gel layer with $CO_2$ carrier was formed on porous PSf and alumina support membranes by filtration of the hydrogel particle suspension. Fig. 4 shows the time course of flux of the aqueous phase of the hydrogel particle suspension, in which glycine and CsOH was dissolved, permeated through the support membranes. As shown in this figure, the initial flux of the carrier solution of the alumina support was higher than that of the PSf support. This result is reasonable because the pore size of the alumina support membrane was larger than that of the PSf support membrane. In this figure, it was also shown that the flux became high when the applied pressure during the filtration process was high. These results indicated that a larger amount of gel particles could be deposited on the alumina support when the filtration was conducted by applying higher pressure. Therefore, it can be expected that the thickness of the gel layer formed on the support membranes could be controlled by changing the pressure during the filtration. On the other hand, instead of the kinds of the support membranes and applied pressure, the flux of the carrier solution became almost the same when filtration was conducted for 20 min. This means that a dense gel particle layers with similar water permeabilities could be formed on the inner surface of the supports within 20 min in all cases.

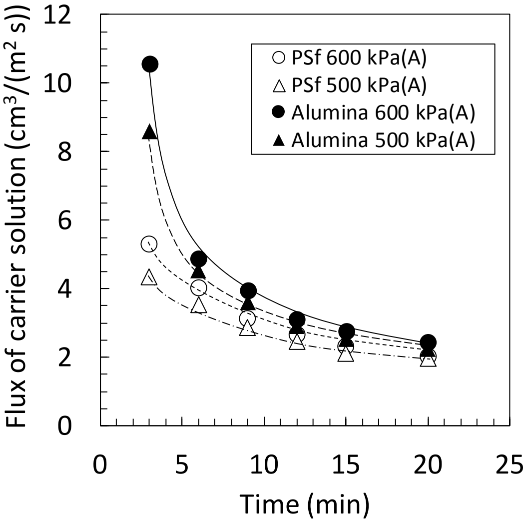

Fig. 4 – Water flux of the membranes with gel layer on alumina and PSf supports prepared at 500 kPa(A) and 600 kPa(A) of applied pressure for gel layer formation

After drying the cylindrical membranes with a layer of the hydrogel particles on the inner surface, the cross-section images of the formed gel layers were observed using FE-SEM. Figs. 5 and 6 are the SEM images of the gel layers on the PSf support membrane and alumina support membrane, respectively, which were formed by applying various pressures during filtration of the gel particle suspension. As clearly shown in these figures, the gel layers formed on both the support membranes were dense and defect free. The gel particles deposited on the support membranes were completely coalesced into a uniform layer. Regarding the difference of the support membranes, the dense layers formed on the alumina support membranes were thicker than those formed on the PSf support membranes. This would be due to the larger solution amount permeated through the support membrane caused by higher carrier solution flux of the alumina support membranes, as indicated in Fig. 4. In addition, as expected from the effect of applied pressure during filtration of gel particle suspension indicated in Fig. 4, the thickness of the dense layer on both of PSf and alumina supports decreased with decreasing the applied pressure. From the SEM images, the dense gel layer thicknesses of the membranes were determined and summarized in Fig. 7. The thickness of the dense layer could be reduced to ca. 4 μm. From these results, it was confirmed that the gel layer could be successfully formed on the inner surface of the cylindrical support membranes by the filtration of the suspension of hydrogel particles and the thickness of two types of the gel layer could be controlled by controlling the applied pressure.

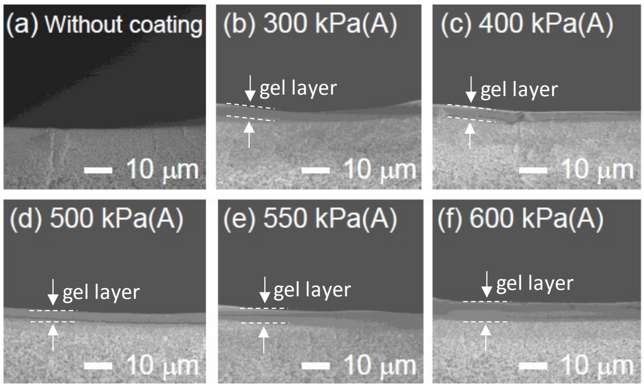

Fig. 5 – SEM images of the cross section of the gel layer formed on the inner surface of the PSf support membrane. Filtration time of hydrogel particle suspension: 20 min.

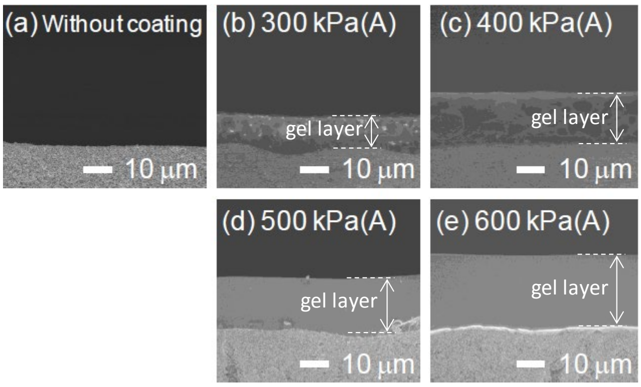

Fig. 6 – SEM images of the cross section of the gel layer formed on the inner surface of the alumina support membrane. Filtration time of hydrogel particle suspension: 20 min.

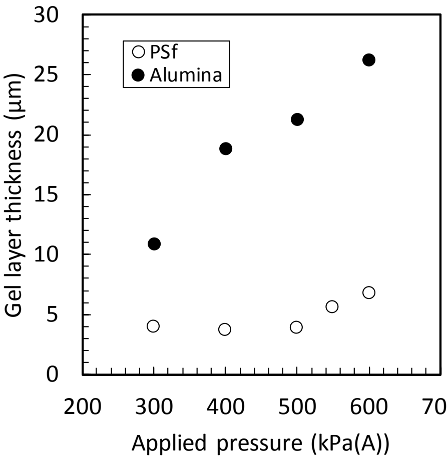

Fig. 7 – Relationship between the gel layer thickness on the surface of the support membrane and applied pressure during gel layer formation process. Filtration time of hydrogel particle suspension: 20 min.

### *3.2. $CO_2$ permeation properties of the cylindrical membranes with gel layer*

Fig. 8 shows the effect of temperature on selective $CO_2$ permeation performances of the cylindrical membranes with a gel layer containing glycine as $CO_2$ carrier. It can be clearly seen that the $CO_2$ permeance of the prepared membranes was much higher than $N_2$ permeance. Therefore, the $CO_2/N_2$ selectivity of the membranes were also high. Furthermore, it can be also seen in Fig. 8(a) that the $CO_2$ permeances of the membrane with $CO_2$ carrier (glycine) were much higher than that of the membrane with no $CO_2$ carrier. It means that the gel layer with glycine permeated $CO_2$ based on facilitated transport mechanism. In addition, the $CO_2$ permeance depended on the temperature more strongly than the $N_2$ permeance. The strong temperature dependence of $CO_2$ permeance was due to the chemical reaction between amino acid and $CO_2$. Because the reaction of amino acid and $CO_2$ is an exothermic reaction (Wei et al., 2014), the $CO_2$ absorption in the membrane decreased with increasing temperature. Therefore, the $CO_2$ permeance of the composite membranes decreased with increasing temperature (Fig. 8(a)). In contrast, because $N_2$ could not react with glycine, $N_2$ permeated through the membrane based on solution-diffusion mechanism. Since $N_2$ was absorbed physically based on Henry's law, the $N_2$ absorption in the membrane was very small under the ambient pressure condition. Therefore, the $N_2$ permeance of the membranes was very low (Fig. 8(b)). The $CO_2$ and $N_2$ permeances of the gel membrane without glycine were also very low and showed no temperature dependence (Fig. 8(a) and (b)).

From the strong temperature dependence of the $CO_2$ permeance, it can be said that the $CO_2$ permeation of these membranes containing glycine were not governed by the solution-diffusion mechanism and would be governed by the facilitated transport mechanism. This means that glycine and CsOH were successfully impregnated in the gel layer and glycine acted as a $CO_2$ carrier. Evaluating the $CO_2$ permeation properties and $CO_2$ separation performance of these membranes, the excellent $CO_2$ permeance of more than $1.75 \times 10^{-4}$ mol/(m$^2$ s kPa), which is equal to 530 GPU and 1960 barrer, and good $CO_2/N_2$ selectivity of more than 1000 were realized at 343 K for the composite membrane with PSf support and the gel layer of which thickness was less than 5 μm. Therefore, it can be said that the developed cylindrical membrane with PSf support could be useful to capture $CO_2$ in flue gases from coal-fired power plant, which has approximately 5–10% $CO_2$ and saturated water vapor at 333–373 K. Here, we compare the $CO_2$ permeation performance of our developed membrane with other cylindrical-type facilitated transport membranes. Kouketsu *et al.* developed a composite membrane composed of PSf ultrafiltration follow fiber as the support, chitosan as the gutter layer and poly(amidoamine) dendrimer as the $CO_2$ carrier (Kouketsu et al., 2007). The $CO_2$ separation layer with approximately 300 nm was formed inner surface of the PSf support membrane. The $CO_2$ permeance of the membrane was approximately $1.6 \times 10^{-7}$ m$^3$(STP)/(m$^2$ s kPa), which equals 21.3 GPU and 6.4 barrer, for $CO_2/N_2$ mixed gas (5/95 vol%) with 100% RH at 313 K. The $CO_2/N_2$ selectivity of the composite membrane was 400. Although their composite membrane had very thin

$CO_2$ separation layer, the $CO_2$ permeance was much lower than that of our membrane because the gutter layer was penetrated in the support membrane. Because we used a hydrogel particle whose size of several tens micron in wet state was much greater than the pore size of the support membranes, penetration of the gel layer was hardly occurred, and thereby the high $CO_2$ permeation was achieved even if the gel layer thickness was much higher than that of the composite membrane developed by Kouketsu *et al*. In another report, Dai *et al*. developed composite membranes with PVA-based thin layer with amino acid salt, such as potassium prolinate and potassium glycinate, on the outer surface of poly(p-phenylene oxide) hollow fiber membrane (Dai et al., 2019). The composite membrane with approximately 500-nm thickness had 791 GPU of $CO_2$ permeance (395.5 barrer of $CO_2$ permeability) for $CO_2/N_2$ mixed gas (10/90 vol%) with 100% RH at room temperature. Owing to the very thin membrane thickness, the $CO_2$ permeance of the composite membrane was higher than that of our membrane. However, the $CO_2$ permeability of our membrane was approximately 5 times higher than the composite membrane developed by Dai *et al*. This means if we can make a composite membrane with thin gel layer of which thickness is 500 nm, the $CO_2$ permeance of our membrane could also be 5 times higher than the composite membrane.

Next, we compare the $CO_2$ permeances of our developed composite membranes with PSf and alumina support membranes. As shown in Fig. 8(a), the membranes with PSf support had higher $CO_2$ permeance than those with alumina support. As indicated in Figs. 5 and 6, the thickness of the gel layers formed on the PSf support were much thinner than that formed on the alumina support. Therefore, it is reasonable that the PSf support based-composite membrane had higher $CO_2$ permeances than alumina based-membrane. On the other hand, the temperature dependences of the $CO_2$ permeances of the two types of composite membranes were different. The $CO_2$ permeances of the membranes with alumina support showed stronger temperature dependence than those with PSf support. This different temperature dependence on the $CO_2$ permeances of the composite membranes with different support membranes suggested that the gel layer formed on each support had different properties. To investigate the difference of the $CO_2$ permeation properties of the gel layers, the $CO_2$ permeabilities, which are the $CO_2$ permeances of the composite membranes normalized with their gel layer thicknesses, were determined and compared with each other.

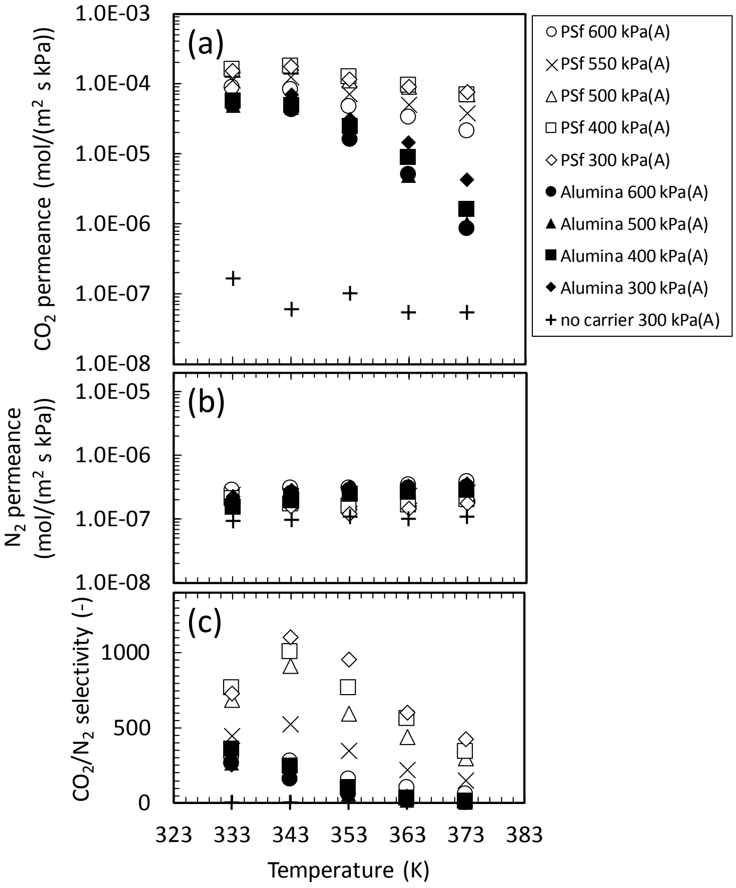

Fig. 8 – Effect of temperature on (a) $CO_2$ permeance, (b) $N_2$ permeance, and (c) $CO_2/N_2$ selectivity of the cylindrical $CO_2$ separation membranes with a gel layer on PSf and alumina supports. Filtration time of hydrogel particle suspension: 20 min.

### *3.3. $CO_2$ permeabilities of the composite membranes*

To investigate the $CO_2$ permeation properties of the gel layers formed on each support membrane, the $CO_2$ permeabilities of the composite membranes were determined. Because the gel layer formed on the support membranes are dense, it could be considered that the rate-determining step of $CO_2$ permeation of the composite membranes are the trans-membrane diffusion of the $CO_2$–glycine complex in the gel layer. Therefore, from the relationship between the $CO_2$ permeance of the composite membranes and reciprocal of thickness of the gel layer, the $CO_2$ permeabilities of the gel layers can be determined. Fig. 9 shows the relationship between the $CO_2$ permeance of the composite membranes at different temperatures and the reciprocal of gel layer thickness. As expected, the plots showed proportional relationship because of the rate-controlling trans-membrane diffusion of the $CO_2$–glycine complex. As shown in Fig. 9, the straight lines for the membranes with different supports had different slopes at the same temperature, this means the two kinds of composite membranes had different $CO_2$ permeabilities at each temperature.

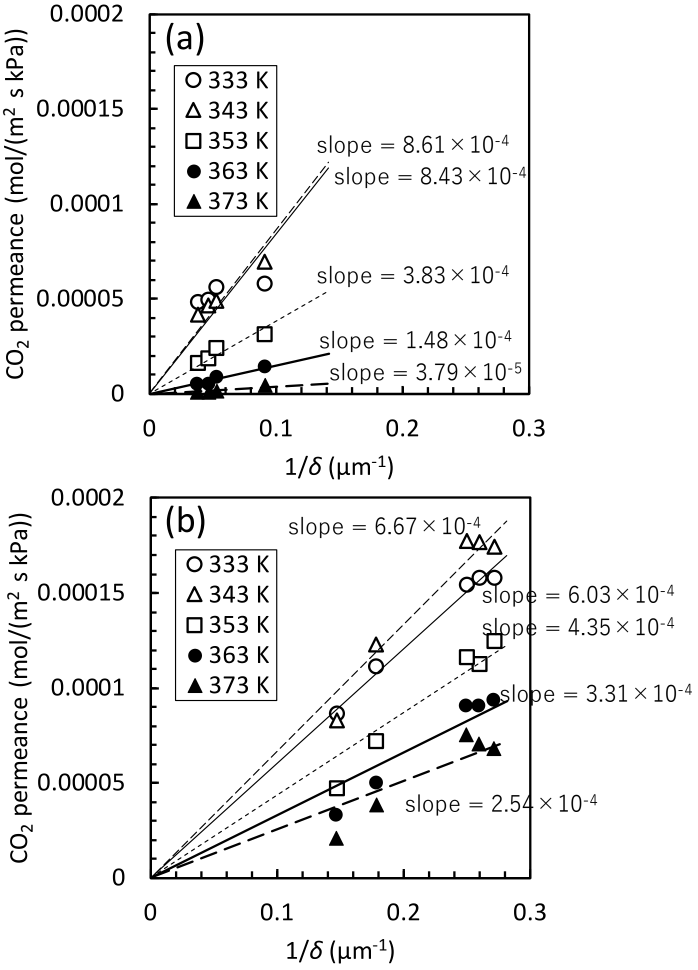

Fig. 9 – Relationship between $CO_2$ permeance of the cylindrical $CO_2$ separation membrane and the reciprocal of thickness of gel layers on (a) alumina support and (b) PSf support

The $CO_2$ permeabilities of the composite membranes determined from the slopes of the straight lines shown in Fig. 9 were plotted against temperature in Fig. 10. As shown in this figure, it can be clearly shown that the temperature dependences of the $CO_2$ permeabilities of each composite membrane were different. The $CO_2$ permeability of the composite membrane with PSf support showed weaker temperature dependence than that of the alumina-based membrane. This result also indicated that the gel layer formed on each support membrane had different properties. In the case of PSf support, the gel layer thickness is thinner (Figs. 5 and 6), however the solution flux of the PSf-based membrane is almost the same as that of the alumina-based support membrane at 20 min filtration (Fig. 4). This means the gel layer deposited on the PSf support is probably denser. This structure of the gel layer would bring about the weaker temperature dependence due to the smaller structure change by the temperature. By contrast, the looser gel layer formed on the alumina support showed the sharp permeability decrease due to the larger structure change. On the other hand, there is another possible consideration on the different $CO_2$ transport properties of the gel membranes formed on the different support membranes. That is about the status of the $CO_2$ carrier (glycine) in the gel layer near the support membranes. Because the interaction between the amine and carboxylic groups on glycine with each type of the support (O=S=O of PSf or under-coordinated surface aluminum atoms) tend to be quite different, it could become an influencing factor for the formation and gas transport properties of the gel layer containing glycine.

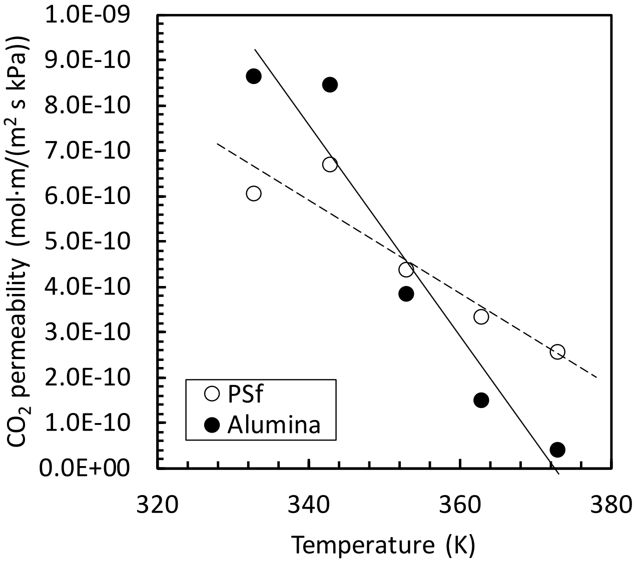

Fig. 10 – Effect of temperature on $CO_2$ permeabilities of the membranes with gel layer on alumina and PSf supports

In the current stage, the critical property of the gel layer that affects the $CO_2$ permeability is not clear. However, it can at least be said that there is a possibility to improve the $CO_2$ permeability of facilitated transport membranes composed of porous support membrane and dense gel layer containing the $CO_2$ carrier by selecting adequate support membrane. To the best of our knowledge, most of researches of facilitated transport membranes were focused on the modification of the $CO_2$ carrier and $CO_2$ separation layer. Based on the results of this study, we would like to propose the development of desirable support membrane as another way to improve the $CO_2$ separation performance of facilitated transport membranes. The development of desirable support membrane includes not only tuning the pore structure, such as porosity, pore size and tortuosity, but also selecting the material, such as polymers with different hydrophilicity and hydrophobicity, ceramics, and metals.

## 4. Conclusion

A dense gel layer containing glycine as the $CO_2$ carrier was formed on two types of porous support membranes: PSf and alumina. The gel layer was formed on the inner surface of the support membrane by forming a cake layer of hydrogel particles composed of hydrophilic PAA/PVA copolymer network and glycine via constant pressure filtration of the hydrogel particle suspension. The gel layer thickness could be controlled by the pressure applied during the constant pressure filtration. Because of the small pore size of the PSf support membrane, the thickness of the gel layer formed on the PSf support was thinner than that formed on the alumina support. Owing to the thin gel layer on the PSf support, the composite membrane composed of the gel layer and PSf support showed higher $CO_2$ permeance than that composed of the gel layer and alumina support at the temperature from 333 to 373 K. This result indicated that the rate-controlling step of $CO_2$ permeation through the gel layer would be trans-membrane diffusion of the $CO_2$–glycine complex and the composite membrane with thinner gel layer could have higher $CO_2$ permeance. On the other hand, the composite membranes with the gel layer on the alumina support membrane had higher $CO_2$ permeability at low temperature up to ca. 350 K. The $CO_2$ permeabilities of the composite membranes with PSf and alumina support membranes showed different temperature dependences. This would be due to the different properties of the gel layer formed on each support membrane. Therefore, it can be said that there is a possibility to improve the $CO_2$ permeability of facilitated transport membranes composed of porous support membrane and dense gel layer containing $CO_2$ carrier by selecting an adequate support membrane.

## References

Baker, R., 2012. Membrane Technology and Applications, Third Edition. Wiley.

Baker, R.W., 2002. Future Directions of Membrane Gas Separation Technology. Ind. Eng. Chem. Res. 41, 1393-1411.

Baker, R.W., Low, B.T., 2014. Gas Separation Membrane Materials: A Perspective. Macromolecules 47, 6999-7013.

Chen, Y., Ho, W.S.W., 2016. High-molecular-weight polyvinylamine/piperazine glycinate membranes for $CO_2$ capture from flue gas. J. Membr. Sci. 514, 376-384.

Chen, Y., Zhao, L., Wang, B., Dutta, P., Winston Ho, W.S., 2016. Amine-containing polymer/zeolite Y composite membranes for $CO_2/N_2$ separation. J. Membr. Sci. 497, 21-28.

Dai, Z., Deng, J., Ansaloni, L., Janakiram, S., Deng, L., 2019. Thin-film-composite hollow fiber membranes containing amino acid salts as mobile carriers for $CO_2$ separation. J. Membr. Sci. 578, 61-68.

Deng, L., Haegg, M.-B., 2010. Swelling behavior and gas permeation performance of PVAm/PVA blend FSC membrane. J. Membr. Sci. 363, 295-301.

Deng, L., Kim, T.-J., Haegg, M.-B., 2009. Facilitated transport of $CO_2$ in novel PVAm/PVA blend membrane. J. Membr. Sci. 340, 154-163.

El-Azzami, L.A., Grulke, E.A., 2009. Carbon dioxide separation from hydrogen and nitrogen. J. Membr. Sci. 328, 15-22.

Han, Y., Wu, D., Ho, W.S.W., 2018. Nanotube-reinforced facilitated transport membrane for $CO_2$/$N_2$ separation with vacuum operation. J. Membr. Sci. 567, 261-271.

Kasahara, S., Kamio, E., Ishigami, T., Matsuyama, H., 2012a. Amino acid ionic liquid-based facilitated transport membranes for $CO_2$ separation. Chem. Commun. (Cambridge, U. K.) 48, 6903-6905.

Kasahara, S., Kamio, E., Ishigami, T., Matsuyama, H., 2012b. Effect of water in ionic liquids on $CO_2$ permeability in amino acid ionic liquid-based facilitated transport membranes. J. Membr. Sci. 415-416, 168-175.

Kim, T.-J., Li, B., Haegg, M.-B., 2004. Novel fixed-site-carrier polyvinylamine membrane for carbon dioxide capture. J. Polym. Sci., Part B: Polym. Phys. 42, 4326-4336.

Kim, T.-J., Vraalstad, H., Sandru, M., Hagg, M.-B., 2013. Separation performance of PVAm composite membrane for $CO_2$ capture at various pH levels. J. Membr. Sci. 428, 218-224.

Kouketsu, T., Duan, S., Kai, T., Kazama, S., Yamada, K., 2007. PAMAM dendrimer composite membrane for $CO_2$ separation: Formation of a chitosan gutter layer. J. Membr. Sci. 287, 51-59.

Matsuyama, H., Terada, A., Nakagawara, T., Kitamura, Y., Teramoto, M., 1999. Facilitated transport of $CO_2$ through polyethylenimine/poly(vinyl alcohol) blend membrane. J. Membr. Sci. 163, 221-227.

Matsuyama, H., Teramoto, M., Matsui, K., Kitamura, Y., 2001. Preparation of poly(acrylic acid)/poly(vinyl alcohol) membrane for the facilitated transport of $CO_2$. J. Appl. Polym. Sci. 81, 936-942.

Moghadam, F., Kamio, E., Matsuyama, H., 2017a. High $CO_2$ separation performance of amino acid ionic liquid-based double network ion gel membranes in low $CO_2$ concentration gas mixtures under humid conditions. J. Membr. Sci. 525, 290-297.

Moghadam, F., Kamio, E., Yoshioka, T., Matsuyama, H., 2017b. New approach for the fabrication of double-network ion-gel membranes with high $CO_2$/$N_2$ separation performance based on facilitated transport. J. Membr. Sci. 530, 166-175.

Moghadam, F., Kamio, E., Yoshizumi, A., Matsuyama, H., 2015. An amino acid ionic liquid-based tough ion gel membrane for $CO_2$ capture. Chem. Commun. 51, 13658-13661.

Qin, Y., Lv, J., Fu, X., Guo, R., Li, X., Zhang, J., Wei, Z., 2016. High-performance SPEEK/amino acid salt membranes for $CO_2$ separation. RSC Adv. 6, 2252-2258.

Rafiq, S., Deng, L., Haegg, M.-B., 2016. Role of Facilitated Transport Membranes and Composite Membranes for Efficient $CO_2$ Capture - A Review. ChemBioEng Rev. 3, 68-85.

Robeson, L.M., 2008. The upper bound revisited. J. Membr. Sci. 320, 390-400.

Tong, Z., Ho, W.S.W., 2017. Facilitated transport membranes for $CO_2$ separation and capture. Sep. Sci. Technol. 52, 156-167.

Wei, C.-C., Puxty, G., Feron, P., 2014. Amino acid salts for CO2 capture at flue gas temperatures. Chem. Eng. Sci. 107, 218-226.

Wu, D., Han, Y., Zhao, L., Salim, W., Vakharia, V., Ho, W.S.W., 2018. Scale-up of zeolite-Y/polyethersulfone substrate for composite membrane fabrication in $CO_2$ separation. J. Membr. Sci. 562, 56-66.

Yegani, R., Hirozawa, H., Teramoto, M., Himei, H., Okada, O., Takigawa, T., Ohmura, N., Matsumiya, N., Matsuyama, H., 2007. Selective separation of $CO_2$ by using novel facilitated transport membrane at elevated temperatures and pressures. J. Membr. Sci. 291, 157-164.

Zhao, Y., Ho, W.S.W., 2012. Steric hindrance effect on amine demonstrated in solid polymer membranes for $CO_2$ transport. J. Membr. Sci. 415-416, 132-138.